wjpmr, 2020,6(6), 34-41

SJIF Impact Factor: 5.922

WORLD JOURNAL OF PHARMACEUTICAL AND MEDICAL RESEARCH

www.wjpmr.com

Research Article

ISSN 2455-3301

WJPMR

ROLE OF MEDICAL BIOPHYSICS MRI IMAGING IN DETECTION OF MASSES IN BREAST CANCER

Hala Moustafa*[1], Metwally Kotb[2] and Diana El-Sherif[3]

[1]Medical Biophysics and Biomedical Equipment's, Faculty of Applied Medical Sciences, October 6 University.
[2]Medical Biophysics, Medical Research Institute, University of Alexandria.
[3]Radiology Departments, Faculty of Applied Medical Sciences.

***Corresponding Author: Hala Moustafa**

Medical Biophysics and Biomedical Equipment's, Faculty of Applied Medical Sciences, October 6 University.

Article Received on 30/03/2020 **Article Revised on 20/04/2020** **Article Accepted on 10/05/2020**

ABSTRACT

Objective: As artificial intelligence methods for the diagnosis of disease advance, we aimed to evaluate machine learning in the predictive task of distinguishing between malignant and benign breast lesions on an independent clinical magnetic resonance imaging (MRI) dataset within a single institution for subsequent use as a computer aid for radiologists. Methods: Between December 2015 and December 2019, 60 female breast patients were enrolled in this study, in addition to 10 control female with a confirmed diagnosis of breast cancer and dense breasts underwent bilateral breast magnetic resonance imaging. In the physics MRI, is effective in the identification of additional masses in dense breasts that are not visualized on mammography. The results: Sensitivity and specificity are the two most important indicators in selection of medical imaging devices for cancer screening. Breast images taken by mammography, and MRI were collected from patients. The statistical features extracted from the histograms of the regions of interest revealed that MRI modality registered the highest scores, and ended with mammography, in the differentiation between normal, benign, and malignant breast tissues. They were then studied and compared for sensitivity and specificity results. The sensitivity and specificity, it is clear that, sensitivity increases on the expense of specificity, and vice versa. The data of this study, revealed that, both mammography and MRI has high sensitivity. In conclusion: The behavior and the general shape of the gray-level histogram describe specific behavior with each category of tissue, namely; normal, benign and malignant, because each modality gives specific shape for each imaged ROI of each tissue category.

KEYWORDS: Physics MRI -Benign Breast Cancer -Malignant Breast Cancer - Photo Shop 7.0 ME Software - MATLAB Software.

INTRODUCTION

Breast cancer is the most common cancer and the second leading cause of cancer death in women in western countries.[1] Breast magnetic resonance imaging (MRI) can demonstrate both ipsilateral and contralateral breast masses that are missed using ultrasound and mammography alone.[2,3] To aid radiologists in diagnostic classification, various investigators are developing computerized image analysis methods for characterization,[4,10] The MRI assessment of breast cancer cases may be hindered by inter-observer and intra-observer variations, labor-intensive interpretation methods, and limited clinical interpretation guidelines.[11,12]

The aim of the work is the application of physics MRI images processing and evaluation techniques for detection and classification of benign and malignant breast Cancer tissues.

MATERIALS AND METHODS

1-Patients

A total of 60 female breast patients were enrolled in this study, in addition to 10 control female (with no symptoms of breast disease). The breast patients were divided into two main groups. One group was of benign breast tumors (30) and the other group of malignant breast changes (20).Patients was diagnosed at the Cairo Scan Women Imaging Units, El-Giza, Egypt. A written informed consent was obtained from each female's patient for performing either the digital mammography or MRI.

2- Procedure of Digital Mammography

During Digital Mammography, the breast is compressed by a dedicated digital mammography machine to even out the tissue, to increase image quality, and to hold the breast still (preventing motion blur). Both front and side images of the breast are taken. Until some years ago,

digital mammography was typically performed with screen-film cassettes. The breast is placed on a special plat form and compressed with a paddle (often made of clear Plexiglas or other plastic). The technologist gradually compresses the breast. The patient was asked to change positions between images. The routine views are a top-to-bottom view (CC view) and an oblique side view (MLO view).[13]

3-Magnetic Resonance Imaging of the breast

A nurse or technologist inserts an intravenous (IV) line into a vein in the hand or arm. The patient was positioned on the moveable examination table. The breast coil is a signal receiver that works with the MRI unit to create the images. The patient IV hooked up to a power injector that drips a saline solution through the IV to prevent blockage of the IV line until the contrast material is injected. The patient would be moved, feet first, into the magnet of the MRI unit and the technologist leaves the room while the MRI examination is performed. The total time spend on the MRI table would be between 30 and 60 minutes.[14-15]

4-Photo Shop 7.0 ME Software

Photo shop 7.0 software is a program that was used to describe the obtained data. The method for the analysis of breast composition was accomplished using transforms pixel values. Pixel uniformity is another important consideration that impacts the accuracy and integrity of the image, which can also influence the presence of noise. Each image was divided into 512 x 512 pixels.

5-Validation Measures

Sensitivity and specificity are statistical measures of the performance of a binary classification test. Sensitivity (also called the true positive rate), measures the proportion of actual positives which are correctly identified as such (e.g. the percentage of sick people who are correctly identified as having the condition). The test results for each subject may or may not match the subject's actual status. In that setting: True positive **(TP)**: Sick people correctly diagnosed as sick False positive **(FP)**: Healthy people incorrectly identified as sick True negative **(TN)**: Healthy people correctly identified as healthy False negative **(FN)**: Sick people incorrectly identified as healthy. Sensitivity relates to the test's ability to identify positive results. The sensitivity of a test is the proportion of people that are known to have the disease who test positive for it.[6]

6-Statistical Analysis

Continuous variables were recorded as mean ± SD; ANOVA-f test, followed by Tukey's test, was used to evaluate the significance of difference ($P < 0.05$) among group. Data were expressed as mean ± standard error (S.E). Data analysis was made by using statistical SPSS - 12 programs for Widows (Chicago, II, USA) when appropriate ($P < 0.05$) was considered statistically significant. Histogram analysis combines techniques that compute statistics and measurements based on the gray-level intensities of the image pixel.

7-MATLAB Software

To calculate the gray-level co-occurrence matrix for a gray scale image, the MATLAB® gray Comtrex [90] package was used to evaluate the following values:

A-Mean

The mean, m of the pixel values in the defined window, estimates the value in the image in which central clustering occurs. The mean can be calculated using the formula:

$$\mu = \frac{1}{MN}\sum_{i=1}^{M}\sum_{j=1}^{N} p(i,j)$$

Where p (i,j) is the pixel value at point (i,j) of an image of size MxN.

B-Standard Deviation

The Standard Deviation, σ is the estimate of the mean square deviation of grey pixel value p (i, j) from its mean value m. It is determined using the formula:

$$\sigma = \sqrt{\frac{1}{MN}\sum_{i-1}^{M}\sum_{j-1}^{N}(p(i,j)-\mu)^2}$$

C-Skewness

Skewness, S characterizes the degree of asymmetry of a pixel distribution in the specified window around its mean. The formula for finding Skewness is given in the below equation:

$$S = \frac{1}{MN}\sum_{i-1}^{M}\sum_{j-1}^{N}\left(\frac{p(i,j)-\mu}{\sigma}\right)^3$$

Where, p (i, j) is the pixel value at point (i,j), m and σ are the mean and standard deviation respectively.

D-Energy

Energy returns the sum of squared elements in the Grey Level Co-Occurrence Matrix (GLCM).The range of energy is [0 1]. Energy is 1 for a constant image. The formula for finding energy is given in below equation:

$$E = \sum_{i,j} P(i,j)^2$$

E-Smoothness

Relative smoothness, R is a measure of grey level contrast that can be used to establish descriptors of relative smoothness. The smoothness is determined using the formula:

$$R = 1 - \frac{1}{1+\sigma^2}$$

Where, σ is the Standard Deviation of the image.

F-Entropy

Entropy is a statistical measure of randomness that can be used to characterize the texture of the input image. Entropy, h can also be used to describe the distribution variation in a region. Overall Entropy of the image can be calculated as:

$$h = -\sum_{k=0}^{L-1} Pr_k(log_2 Pr_k)$$

Where, Pr is the probability of the k-the grey level, which can be calculated as Zk /m*n, Zk is the total number of pixels with the k-the grey level and L is the total number of grey levels.

G-Kurtosis

Kurtosis, K measures the Peakness or flatness of a distribution relative to a normal distribution. The conventional definition of kurtosis is:

$$K = \left\{\frac{1}{MN}\sum_{i=1}^{M}\sum_{j=1}^{N}\left[\frac{p(i,j)-\mu}{\sigma}\right]^4\right\} - 3$$

Where, p (i,j) is the pixel value at point (i,j), m and σ are the Mean and Standard Deviation respectively. The -3 term makes the value zero for a normal distribution.

H- Root Mean Square (RMS)

The RMS (Root Mean Square) computes the RMS value of each row or column of the input, along vectors of a specified dimension of the input, or of the entire input. The RMS value of the jth column of an M-by-N input matrix u is given by below equation:

$$y = \sqrt{\frac{\Sigma_{i=1}^{M}|u_{ij}|^2}{M}}$$

I- Inverse Difference Moment (IDM)

It is a measure of image texture. IDM ranges from 0.0 for an image that is highly textured to 1.0 for an image that is un textured. The formula for finding the IDM is given in below equation:

$$H = \sum_{i,j}\frac{P(i,j)}{1+|i-j|}$$

J-Contrast

Contrast returns a measure of the intensity contrast between a pixel and its neighbour over the whole image. The range of Con-trast is [0 (size (GLCM, 1)-1) x2]. Contrast is 0 for a constant image. Contrast is calculated by using the equation given below:

$$C = \sum_{i,j}|i-j|^2 P(i,j)$$

K- Correlation

Correlation returns a measure of how correlated a pixel is to its neighbor over the whole image. The range of correlation is [-1 1]. Correlation is 1 or -1 for a perfectly positively or negatively correlated image. Correlation is NaN (Not a Number) for a constant image. The below equation shows the calculation of Correlation.

$$Corr = \sum_{i,j}\frac{(i-\mu_i)(j-\mu_j)P(i,j)}{\sigma_i\sigma_j}$$

Where μi, μj, σi, σj, and are the means and standard deviations of Pi and Pj, the partial probability density functions.

L- Homogeneity

Homogeneity returns a value that measures the closeness of the distribution of elements in the GLCM to the GLCM diagonal. The range of Homogeneity is [0 1]. Homogeneity is 1 for a diagonal GLCM. The Homogeneity is evaluated using the equation:

$$H = \sum_{i,j}\frac{P(i,j)}{1+|i-j|}$$

M- Variance

Variance is the square root of standard deviation. The formula for finding Variance is:

RESULTS

Figure (1-2&3): Some representative breast MRI studies from the independent consecutive test set as classified by the trained MRI machine learning system are presented in Fig.

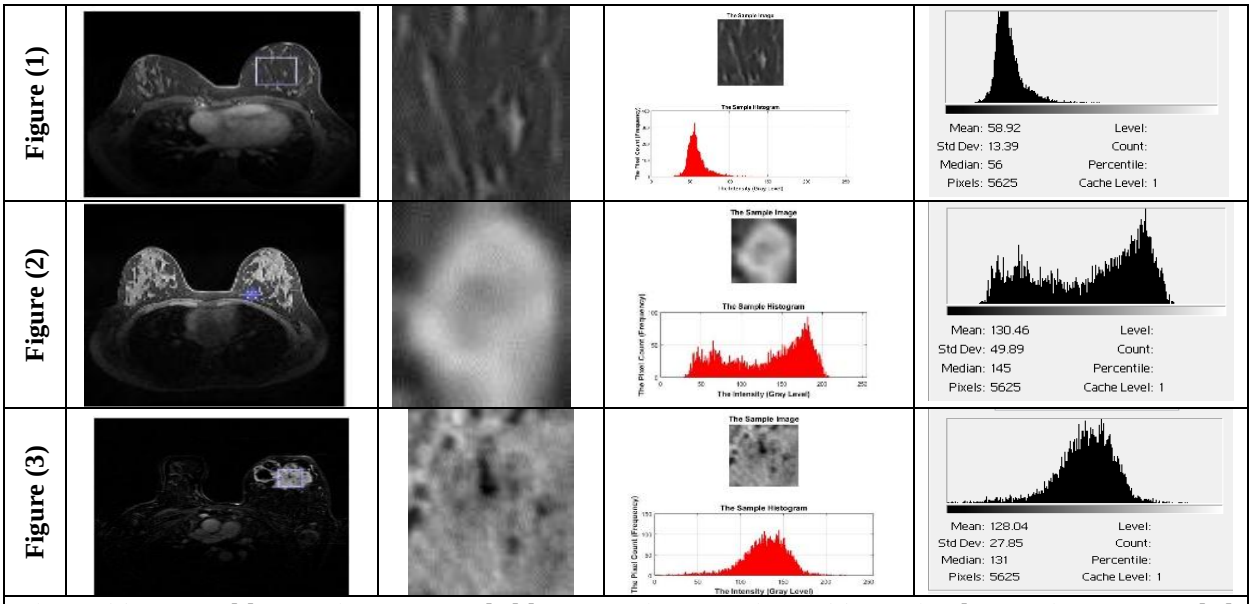

Figure (1): Normal breast tissues, recorded by MRI Siemens. Figure (2): Benign breast tissues, recorded by MRI Siemens. Figure (3): Malignant breast tissues, recorded by MRI Siemens.

Table (1): Comparison between the three studied groups according to Mean, Standard Deviation & Coefficient of Variation of different parameters using Photoshop program.

Mean	Normal	Benign	Malignant	F	p	Pairwise comparison		
						p_1	p_2	p_3
MRI	67.98±13.64	123.8±17.56	91.51±30.38	21.068*	<0.001*	<0.001*	0.030*	<0.001*
CC	180.0±22.70	153.4±33.84	154.0±27.87	2.856	0.066	-	-	-
MLO	176.9±22.93	158.7±33.68	152.5±27.88	2.134	0.127	-	-	-
Standard deviation	**Normal**	**Benign**	**Malignant**	**F**	**p**	**Pairwise comparison**		
						p_1	p_2	p_3
MRI	14.20±2.87	43.06±13.87	31.01±11.90	20.575*	<0.001*	<0.001*	0.001*	0.005*
CC	4.79 ± 1.71	19.45±11.11	17.96 ± 6.62	9.648*	<0.001*	<0.001*	0.002*	0.829
MLO	5.69 ± 1.60	18.23± 11.10	17.64 ± 9.21	6.855*	0.002*	0.002*	0.007*	0.975
Coefficient of Variation	**Normal**	**Benign**	**Malignant**	**F**	**p**	**Pairwise comparison**		
						p_1	p_2	p_3
MRI	65.20±14.07	128.1±19.02	88.09±32.15	24.954*	<0.001*	<0.001*	0.051	<0.001*
CC	176.6±22.13	152.9±35.60	153.2±29.32	2.069	0.136	-	-	-
MLO	176.8±23.04	158.0±35.09	151.3±29.64	2.126	0.128	-	-	-

Table (2): Comparison between the three studied groups according to Mean, Standard Deviation & Coefficient of Variation of different parameters using MATLAB program.

Mean	Normal	Benign	Malignant	F	p	Pairwise comparison		
						p_1	p_2	p_3
MRI	0.22 ± 0.06	0.35 ± 0.10	0.36 ± 0.15	5.428*	0.007*	0.015*	0.008*	0.972
CC	0.03 ± 0.01	0.14 ± 0.11	0.12 ± 0.06	6.515*	0.003*	0.002*	0.019*	0.674
MLO	0.03 ± 0.01	0.13 ± 0.10	0.13 ± 0.08	5.089*	0.009*	0.008*	0.025*	0.965
Standard Deviation	**Normal**	**Benign**	**Malignant**	**F**	**p**	**Pairwise comparison**		
						p_1	p_2	p_3
MRI	50.49±22.14	123.7±17.19	88.10±26.51	66.566*	<0.001*	<0.001*	<0.001*	<0.001*
CC	175.3±20.84	159.5±33.98	151.4±27.82	2.232	0.115	-	-	-
MLO	176.8±22.83	164.3±32.55	151.5±27.45	2.521	0.087	-	-	-
Coefficient of Variation	**Normal**	**Benign**	**Malignant**	**F**	**p**	**Pairwise comparison**		
						p_1	p_2	p_3
MRI	19.52±7.99	43.55±13.65	30.74±12.11	28.385*	<0.001*	<0.001*	0.002*	0.001*
CC	4.78±1.52	17.98±10.54	17.65±6.85	10.562*	<0.001*	<0.001*	<0.001*	0.989
MLO	5.67 ± 1.65	17.45 ±10.93	17.43 ± 9.03	6.326*	0.003*	0.003*	0.007*	1.000

Table (3): Comparison between the three studied groups according to Median Coefficient of Variation, Maximum Value, Minimum Value Skewness of different parameters using MATLAB program.

Median	Normal	Benign	Malignant	F	p	Pairwise comparison		
						p_1	p_2	p_3
MRI	46.83±24.14	127.2±18.88	84.57±28.27	68.115*	<0.001*	<0.001*	<0.001*	<0.001*
CC	174.8±20.98	158.9±35.57	150.7±29.38	2.087	0.132	-	-	-
MLO	176.5±22.93	163.5±34.27	150.5±29.08	2.415	0.096	-	-	-
Coefficient of variation	**Normal**	**Benign**	**Malignant**	**F**	**p**	**Pairwise comparison**		
						p_1	p_2	p_3
MRI	0.45 ± 0.21	0.35 ± 0.10	0.36 ± 0.15	2.385	0.100	-	-	-
CC	0.03 ± 0.01	0.13 ± 0.10	0.12 ± 0.06	6.674*	0.002*	0.002*	0.007*	0.969
MLO	0.03 ± 0.01	0.12 ± 0.10	0.12 ± 0.08	4.363*	0.016*	0.015*	0.028*	0.997
Maximum value	**Normal**	**Benign**	**Malignant**	**F**	**p**	**Pairwise comparison**		
						p_1	p_2	p_3
MRI	141.3 ± 25.34	203.7 ± 31.8	187.5 ± 55.24	18.247*	<0.001*	<0.001*	<0.001*	0.358
CC	194.2 ± 21.57	223.08 ± 25.6	208.3 ± 30.84	5.663*	0.005*	0.007*	0.333	0.108
MLO	197.9 ± 24.32	223.2 ± 24.4	202.15 ± 24.26	7.795*	0.001*	0.011*	0.895	0.005*
Minimum value	**Normal**	**Benign**	**Malignant**	**F**	**P**	**Pairwise comparison**		
						p_1	p_2	p_3
MRI	12.43 ± 14.93	12.43 ± 14.9	12.4 ± 14.93	8.818*	<0.001*	0.001*	0.414	0.024
CC	11.90 ± 12.22	11.90 ± 12.2	11.90 ± 12.22	7.208*	0.001*	0.005*	0.001*	0.620
MLO	162.55 ± 21.3	162.5 ± 21.3	162.5 ± 21.35	5.617*	0.005*	0.026*	0.004*	0.356
Skevness value	**Normal**	**Benign**	**Malignant**	**F**	**p**	**Pairwise comparison**		
						p_1	p_2	p_3
MRI	0.79 ± 0.76	0.79 ± 0.76	0.79 ± 0.76	27.927*	<0.001*	<0.001*	<0.001*	0.123
CC	0.81 ± 0.88	0.81 ± 0.88	0.81 ± 0.88	1.277	0.285	-	-	-
MLO	1.19 ± 0.64	1.19 ± 0.64	1.19 ± 0.64	0.254	0.776	-	-	-

Table (4): Comparison between the three studied groups according to Entropy, Mode value, Kurtosis, Percentile 25, Percentile 75 of different parameters using MATLAB program

Entropy value	Normal	Benign	Malignant	F	p	Pairwise comparison		
						p_1	p_2	p_3
MRI	0.05 ± 0.07	0.0 ± 0.002	0.001 ± 0.00	9.721*	<0.001*	0.001*	0.001*	0.998
CC	0.0 ± 0.0	0.0 ± 0.0	0.0 ± 0.0	-	-	-	-	-
MLO	0.0 ± 0.0	0.0 ± 0.0	0.0 ± 0.0	-	-	-	-	-
Mode value	**Normal**	**Benign**	**Malignant**	**F**	**p**	**Pairwise comparison**		
						p_1	p_2	p_3
MRI	42.62 ± 28.55	122.90 ± 50.89	77.14 ± 34.48	27.136*	<0.001*	<0.001*	0.006*	0.001*
CC	174.09 ± 21.30	161.26 ± 38.82	152.59 ± 32.80	1.407	0.252	-	-	-
MLO	175.80 ± 24.28	162.39 ± 38.37	150.75 ± 32.23	1.751	0.181	-	-	-
Kurtosis value	**Normal**	**Benign**	**Malignant**	**F**	**p**	**Pairwise comparison**		
						p_1	p_2	p_3
MRI	5.57 ± 2.73	1.95 ± 0.27	3.64 ± 1.34	22.507*	<0.001*	<0.001*	0.002*	0.014*
CC	3.50 ± 1.21	3.61 ± 2.32	3.08 ± 0.87	0.599	0.552	-	-	-
MLO	3.01 ± 0.45	3.27 ± 1.79	2.79 ± 0.53	0.811	0.448	-	-	-
Percentile 25	**Normal**	**Benign**	**Malignant**	**F**	**p**	**Pairwise comparison**		
						p_1	p_2	p_3
MRI	36.86 ± 22.09	85.76 ± 19.14	66.71 ± 27.86	28.315*	<0.001*	<0.001*	<0.001*	0.026*
CC	172.0 ± 20.97	147.08 ± 39.07	139.36 ± 30.19	3.394*	0.039*	0.093	0.032*	0.680
MLO	172.80 ± 23.0	152.22 ± 38.24	139.14 ± 31.14	3.124*	0.050*	0.216	0.040*	0.347
Percentile 75	**Normal**	**Benign**	**Malignant**	**F**	**p**	**Pairwise comparison**		
						p_1	p_2	p_3
MRI	60.80 ± 25.45	161.15 ± 23.73	106.14 ± 29.44	89.331*	<0.001*	<0.001*	<0.001*	<0.001*
CC	178.18 ± 20.43	170.58 ± 31.52	163.45 ± 26.80	1.018	0.367	-	-	-
MLO	180.40 ± 22.78	174.74 ± 29.83	163.50 ± 25.53	1.582	0.213	-	-	-

Table (5): Comparison between the three studied groups according to Contrast, Energy ,Homogeneity ,IDM of different parameters using MATLAB program.

Contrast	Normal	Benign	Malignant	F	p	Pairwise comparison		
						p_1	p_2	p_3
MRI	0.64 ± 1.11	0.0 ± 0.01	0.01 ± 0.02	6.772*	0.002*	0.008*	0.008*	1.000
CC	0.0 ± 0.0	0.0 ± 0.0	0.0 ± 0.0	-	-	-	-	-
MLO	0.0 ± 0.0	0.0 ± 0.0	0.0 ± 0.0	-	-	-	-	-
Energy	**Normal**	**Benign**	**Malignant**	**F**	**p**	**Pairwise comparison**		
						p_1	p_2	p_3
MRI	0.97 ± 0.04	1.0 ± 0.0	1.0 ± 0.0	7.037*	0.002*	0.006*	0.007*	1.000
CC	1.0 ± 0.0	1.0 ± 0.0	1.0 ± 0.0	-	-	-	-	-
MLO	1.0 ± 0.0	1.0 ± 0.0	1.0 ± 0.0	-	-	-	-	-
Homogeneity	**Normal**	**Benign**	**Malignant**	**F**	**p**	**Pairwise comparison**		
						p_1	p_2	p_3
MRI	0.99 ± 0.02	1.0 ± 0.0	1.0 ± 0.0	6.772*	0.002*	0.008*	0.008*	1.000
CC	1.0 ± 0.0	1.0 ± 0.0	1.0 ± 0.0	-	-	-	-	-
MLO	1.0 ± 0.0	1.0 ± 0.0	1.0 ± 0.0	-	-	-	-	-
IDM	**Normal**	**Benign**	**Malignant**	**F**	**p**	**Pairwise comparison**		
						p_1	p_2	p_3
MRI	10470.1±5674.6	29595.3±4229.	19932.9±6265.0	74.593*	<0.001*	<0.001*	<0.001*	<0.001*
CC	39228.4±4526.8	36812.6±7417.	34514.9±6346.7	1.898	0.158	-	-	-
MLO	39981.1±5035.2	38021.0±6918.	34845.8±5967.3	2.562	0.084	-	-	-

DISCUSSION

Breast MRI is an expensive method, with potential false positive results and high frequency of incidental findings that may require further investigation. A thorough diagnostic evaluation with mammography and US must be undertaken before considering the necessity of MRI.[17] According to the recommendations of the European Society of Breast Cancer Specialists, breast MRI should be performed in radiological centers specialized in conventional breast imaging (mammography and US), percutaneous biopsy and MRI-directed second-look US.[18]

At the same time, more range, and consequently, more area is occupied by the benign breast tissues due to the wide variations in the benign breast tissues, especially because the types of benign breast tumors are numerous including fibro adenomas, Periductal mastitis, Fat necrosis, Lobular neoplasia, fibrocystic change, areas of thickening, and others.[19-20] The peak(s) is characterized by broad base and broad peak with relatively lower height in comparison to the peak and shape of the normal breast tissue. Malignant breast tissue appears as a peak of gradual increase in intensity forming a sharp peak of high gray-level at the high end of the histogram but declined sharply towards the lower end of the histogram forming an extended tail towards the lower end of the histogram. The distribution curve is skewed to left which is called (-) skewed **Figure (1, 2&3).**

The intensity measurements measure the gray-scale statistics in the ROIs. In the present work, typical intensity measurements included 17 statistical features as follows: mean, standard deviation, median, coefficient of variation, maximum values, minimum values, skewness, entropy, mode value, kurtosis, 25th-percentile, 75th-percentile, contrast, energy, and homogeneity, IDM, and RMS value. Due to the numerous statistical features extracted from the gray-level histograms, consequently, from the ROIs, and as a trial to obtain a solid conclusion concerning the most suitable modality to be able to choose the modality that gives the most accurate breast lesion diagnosis, a score table was established. Also, it is scored to point 2 if two significant differences exist, e.g., normal/benign, benign/malignant, and it is scored to point 3 if three significant differences exist, e.g., normal/benign, normal/malignant, and benign/malignant. Normal breast tissue appears as a sharp peak of high gray-level at the lower end of the histogram, with positive kurtosis.[21-22]

The COV is the best feature to be used to differentiate between normal and malignant breast tissues using Photoshop 7.0 ME software. When comparing variability between data sets with different measurement scales or very different mean values. In medical imaging machines, gain (amount of amplification or attenuation of the information signal) is optimized by the operator. Gain Knob (Controls overall brightness of the image). Time Gain Compensation (TGC) (Allows adjustment of image brightness at selective depth. The differentiation between benign and malignant breast tissues represents utmost importance. It is clear from tables, that using photoshop 7.0 ME software, MRI registers the unique modality that may be used to differentiate between these two categories of breast tissues. Sensitivity and specificity are the two most important indicators in selection of medical imaging devices for cancer screening. Breast images taken by mammography, and MRI were collected from 78 patients. They were then studied and compared for sensitivity and specificity

results. The sensitivity and specificity, it is clear that, sensitivity increases on the expense of specificity, and vice versa. The data of this study, revealed that, both mammography and MRI has high sensitivity. This is because the acoustic characteristics of benign and malignant lesions are overlapping. This study showed high sensitivity of MRI for differentiation as the study of.[23] Results showed that no imaging method has perfect sensitivity and perfect specificity for the diagnosis of breast cancer.

CONCLUSION

The histogram of normal breast tissue appears as sharp peak, leptokurtic, located at the high end of the gray-scale in case of mammography, and at the lower end of the gray-scale in case of MRI, with (-) skewness.The histogram of benign breast tissue appears as a broad peak at the middle of the gray-scale, with broad base and sharp top with more range and more area is occupied by the histogram distribution in case of mammography. In case of MRI, the benign histogram gray level distribution is characterized by two main peaks at the beginning and at the end of the distribution with the distribution is located in the middle of the gray-scale with peaks and valleys. The histogram of malignant breast tissue appears as a broad peak at the middle of the gray-scale, with broad base and broad top, with (-) skewness, in case of mammography. While, in case of MRI, the histogram appears as a peak of gradual increase in intensity forming a sharp peak at the lower end of the histogram but declined sharply towards the high end of the histogram forming an extended tail towards the lower end of the gray-scale, with (-) skewness. In the quantitative comparisons, the statistical features extracted from the histograms of the regions of interest revealed that MRI modality registered the highest scores, and ended with mammography, in the differentiation between normal, benign, and malignant breast tissues. The sensitivity and specificity as evaluation measures, the results revealed that, both mammography and MRI has high sensitivity.

REFERENCES

1. Siegel RL, Miller KD, Jemal A. Cancer statistics, 2018. CA Cancer J Clin, 2018; 68(1): 7–30.
2. Orel SG, Schnall MD. MR imaging of the breast for the detection, diagnosis, and staging of breast cancer. *Radiology*, 2001; 220(1): 13-30.
3. Liberman L, Mortis EA, Kim CM, Kaplan JB, Abramson AF, Menell JH, et al. MR imaging findings in the contralateral breast of women with recently diagnosed breast cancer. *Am J Roentgenol*, 2003; 180: 333-41.
4. Giger ML, Chan HP, Boone J. Anniversary paper: history and status of CAD and quantitative image analysis: the role of medical physics and AAPM. Med Phys, 2008; 35(12): 5799–820.
5. Giger ML, Karssemeijer N, Schnabel JA. Breast image analysis for risk assessment, detection, diagnosis, and treatment of Cancer. Annu Rev Biomed Eng, 2013; 15(1): 327–57.
6. Chen W, Giger ML, Lan L, et al. computerized interpretation of breast MRI: investigation of enhancement-variance dynamics. Med Phys, 2004; 31(5): 1076–82.
7. Li H, Zhu Y, Burnside ES, et al. Quantitative MRI radionics in the prediction of molecular classifications of breast cancer subtypes in the TCGA/TCIA data set. NPJ Breast Cancer, 2016; 2: 16012.
8. Antropova N, Abe H, Geiger ML. Use of clinical MRI maximum intensity projections for improved breast lesion classification with deep CNNs. J MedImaging (Bellingham), 2018; 5(1): 014503.
9. Gallego-Ortiz C, Martel AL. A graph-based lesion characterization and deep embedding approach for improved computer-aided diagnosis of non-mass breast MRI lesions. Med Image Anal, 2019; 51: 116–24.
10. Parekh VS, Jacobs MA. Integrated radiomic framework for breast cancer and tumor biology using advanced machine learning and multipara metric MRI. NPJ Breast Cancer, 2017; 3: 43.
11. Mussurakis S, Buckley DL, Coady AM, et al. Observer variability in the interpretation of contrast enhanced MRI of the breast. Br J Radiol, 1996; 69(827): 1009–16.
12. Kim SJ, Morris EA, Liberman L, et al. Observer variability and applicability of BI-RADS terminology for breast MR imaging: invasive carcinomas as focal masses. AJR Am J Roentgenol, 2001; 177(3): 551–7.
13. Bick U Full-field digital mammography. Fortschr Röntgenstr, 2000; 172: 957–964.
14. Jacobs MA, Barker PB, Bluemke DA, et al. Benign and malignant breast lesions: diagnosis with multiparametric MR imaging. *Radiology*, 2003; 229: 225- 232.
15. Shahar KH, Solaiyappan M, Bluemke DA. Quantitative differentiation of breast lesions based on threedimensional morphology from magnetic resonance imaging. *J Comput Assist Tomogr*, 2002; 26: 1047-1053.
16. Teller P, Jefford VJ, Gabram SG, et al. The utility of breast MRI in the management of breast cancer. Breast J., 2010; 16: 394-403.
17. American College of Radiology. Breast Imaging Reporting and Data System: BI-RADS Atlas. 4th ed. Reston, VA: American College of Radiology, 2003.
18. Moy L, Elias K, Patel V, et al. Is breast MRI helpful in the evaluation of inconclusive mammographic findings? AJR Am J Roentgenol, 2009; 193: 986-93.
19. Downey K, Riches SF, Morgan VA, Giles SL, Attygalle AD, Ind TE, et al. Relationship between imaging biomarkers of stage I cervical cancer and poor-prognosis histologic features: quantitative histogram analysis of diffusion-weighted MR images. AJR Am J Roentgenol, 2013; 200(2): 314-20.

20. Figueroa JD, Pfeiffer RM, Brinton LA, Palakal MM, Degnim AC, Radisky D et al. Standardized measures of lobular involution and subsequent breast cancer risk among women with benign breast disease: a nested case-control study. Breast Cancer Research & Treatment, 2016; 159(1): 163-72.
21. National Cancer Institute. Breast Cancer Treatment During Pregnancy (PDQ). 2019. Accessed at www.cancer.gov/types/breast/hp/pregnancy-breast-treatmentpdq#section/all on August 26, 2019.
22. Venkataraman S, Slanetz PJ. Breast imaging for cancer screening: Mammography and ultrasonography. Up To Date. 2019. Accessed at https://www.uptodate.com/contents/breast-imaging-for-cancer- screeningmammography-and-ultrasonography on August 26, 2019.
23. Ganesh N. Sharma, Rahul Dave, Jyotsana Sanadya, Piush Sharma, and K. K Sharma. Various types and management of breast cancer: an overview. J Adv Pharm Technol Res., 2010; 1(2): 109–26.